Electronic Supplementary Information

Discovery of a quorum sensing modulator pharmacophore by 3D small-molecule microarray screening

David M. Marsden, Rebecca L. Nicholson, Mette E. Skindersoe, Warren R. J. D. Galloway, Hannah F. Sore, Michael Givskov, George P. C. Salmond, Mark Ladlow, Martin Welch and David R. Spring*

**Department of Chemistry, University of Cambridge, Lensfield Road, Cambridge, UK CB2 1EW*

*E-mail: spring@ch.cam.ac.uk

A – Synthesis of the library

General information

Experimental techniques and apparatus as standard except as otherwise indicated. Reactions were carried out under nitrogen with dry, freshly distilled solvents. Dichloromethane (DCM) was distilled from calcium hydride. Diethyl ether and tetrahydrofuran (THF) were freshly distilled from sodium benzophenone ketyl under argon. All other reagents were purifed in accordance with the instructions in "Purifcation of Laboratory Chemical" or used as obtained from commercial sources (Aldrich, unless stated otherwise). Yields refer to chromatographically and spectroscopically pure compounds. All reactions were monitored by thin layer chromatography (TLC) using glass plates precoated with Merck silica gel 60 F254 or aluminum oxide 60 F254. Visualisation was carried out using UV uorescence (l = 254 nm) or by staining with ammonium molybdate or potassium permanganate. Retention factors (R_f) are quoted to two decimal places. Melting points were obtained using a Reichert hot plate microscope with a digital thermometer attachment and are uncorrected. Infrared spectra were recorded neat on a Perkin-Elmer Spectrum One spectrometer with internal referencing. Absorption maxima (max) are reported in wavenumbers (cm^{-1}) and the following abbreviations are used: w, weak; md, medium; st, strong; br, broad. Proton magnetic resonance spectra were recorded on Bruker

Ultrashield 400 or 500 MHz spectrometers. Proton assignments are supported by 1H-1H spectra where necessary. Chemical shifts (^{1}H-NMR: d) are quoted in ppm and are referenced to the residual non-deuterated solvent peak. Chemical shifts were measured relative to chloroform (1H d 7.26, 13C d 77.36), methanol (1H d 3.34, 13C d 49.86) or DMSO (1H d 2.54, 13C d 40.45) as appropriate. Coupling constants (*J*) are reported to the nearest 0.5 Hz. Data are reported as follows: chemical shift, integration, multiplicity [br, broad; s, singlet; d, doublet; t, triplet; q, quartet; quin, quintet; sext, sextuplet; sept, septuplet; m, multiplet; or as a combination of these (e.g. dd, dt, etc.)], coupling constant(s) and assignment. Carbon magnetic resonance spectra were recorded on Bruker Ultrashield 400 or 500 MHz spectrometers. Carbon spectra assignments are supported by DEPT editing. Chemical shifts (^{13}C-NMR: d) are quoted in ppm to the nearest 0.1 ppm, and are referenced to the deuterated solvent. LCMS spectra were recorded on an HP/Agilent LCMS APCI 120-1000 full gradient machine. High resolution mass measurements were made by the EPSRC mass spectrometry service (Swansea) on a Finnigan MAT 95XP spectrometer or the departmental Waters LCT machine.

- The synthesis of the library is based on Scheme 2 in the main paper. DIC (6.31 mL, 40.75 mmol), DMAP (747 mg, 6.11 mmol) and 6-[2-(2-N-Boc-amino-ethoxy)-ethoxy]-hexanoic acid **14** (3.25 g, 10.19 mmol) were added sequentially to a solution of PL-TFP resin (Polymer Laboratories - tetrauorophenol beads) suspended in anhydrous DCM (150 mL) and agitated for 18 hours at room temperature. The beads were filtered, washed with DCM (x 5) and then dried under vacuum. The compound loading on the beads was determined as 10 mmol/g.
- The beads (80 mg, 0.08 mmol) were re-suspended in DMF and amines **A1-A95** (0.08 mmol, Figure 1 & 2) were added to individual vials containing the suspension of beads. The reaction mixtures were heated at 60 ^{o}C for 18 hours, filtered, washed with DMF and the filtrates evaporated under vacuum. The presence of the required amides **LP1-LP95** was confirmed by LCMS (APCI^{+}). Samples prepared from amino benzophenones **A34**, **A82** and **A83** were unsuccessful.
- The amide library was deprotected by treatment with HCl in EtOAc at room temperature. Following removal of excess HCl/EtOAc under vacuum, samples were re-dissolved in DMF to a concentration of approximately 10 mM, deprotonated using Amberlyst-21 resin to give amines **L1-L95**. Ligands were finally microarrayed using the method described in the experimental section of the main paper.

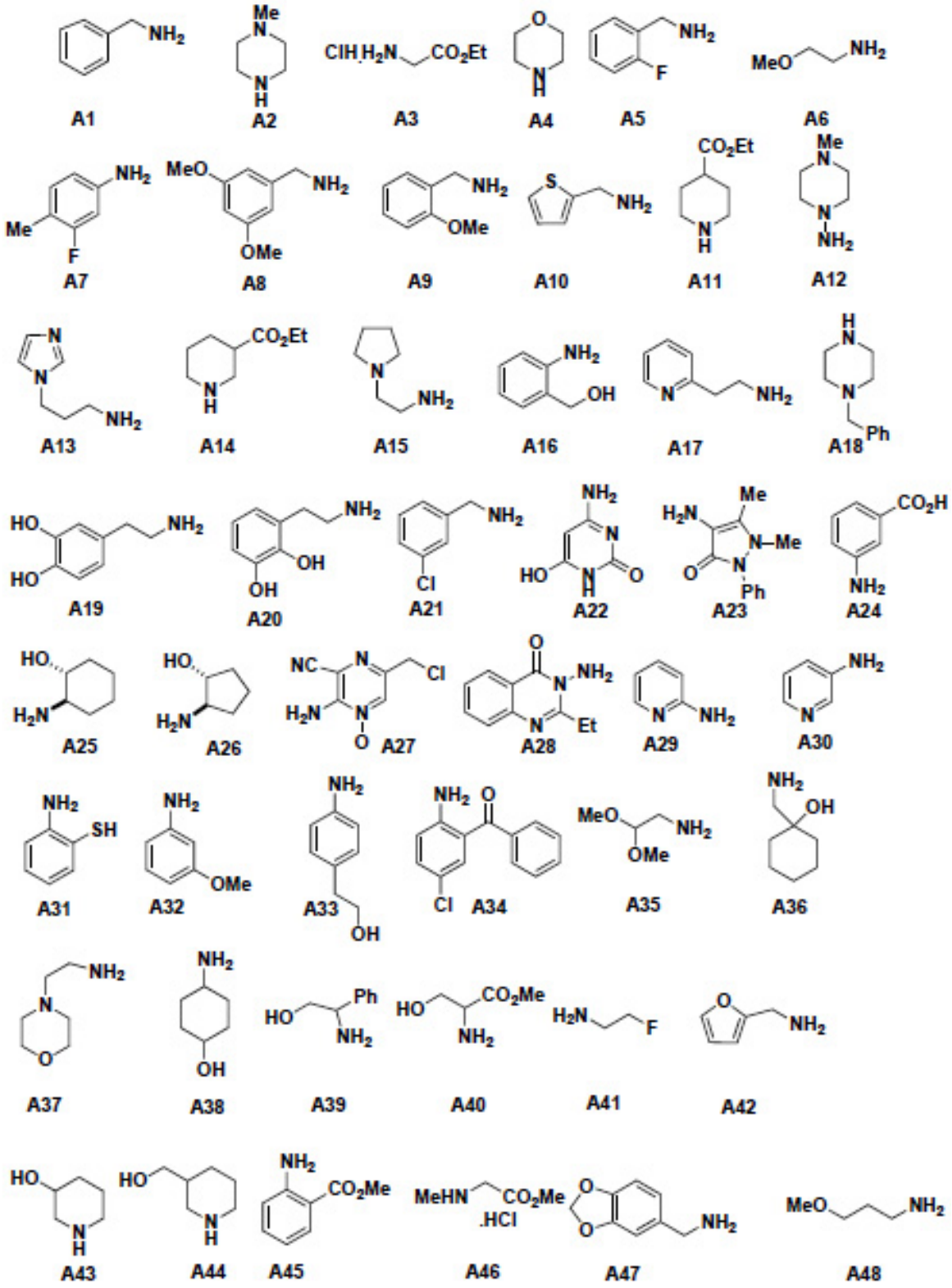

Figure 1 List of amines **A1-A48**

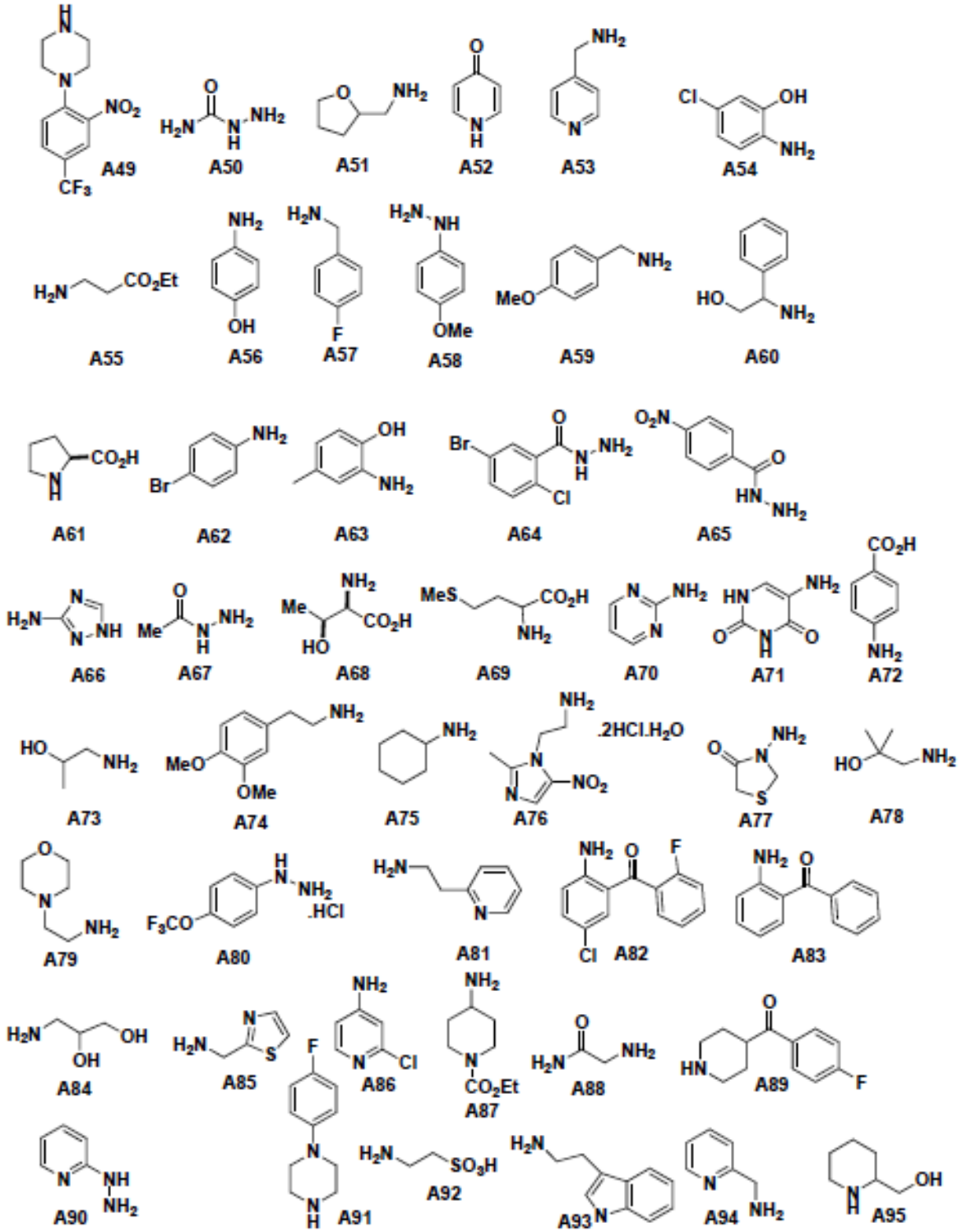

Figure 2 List of amines **A49-A95**

B – Microarraying data

B1 – AHL linker scans

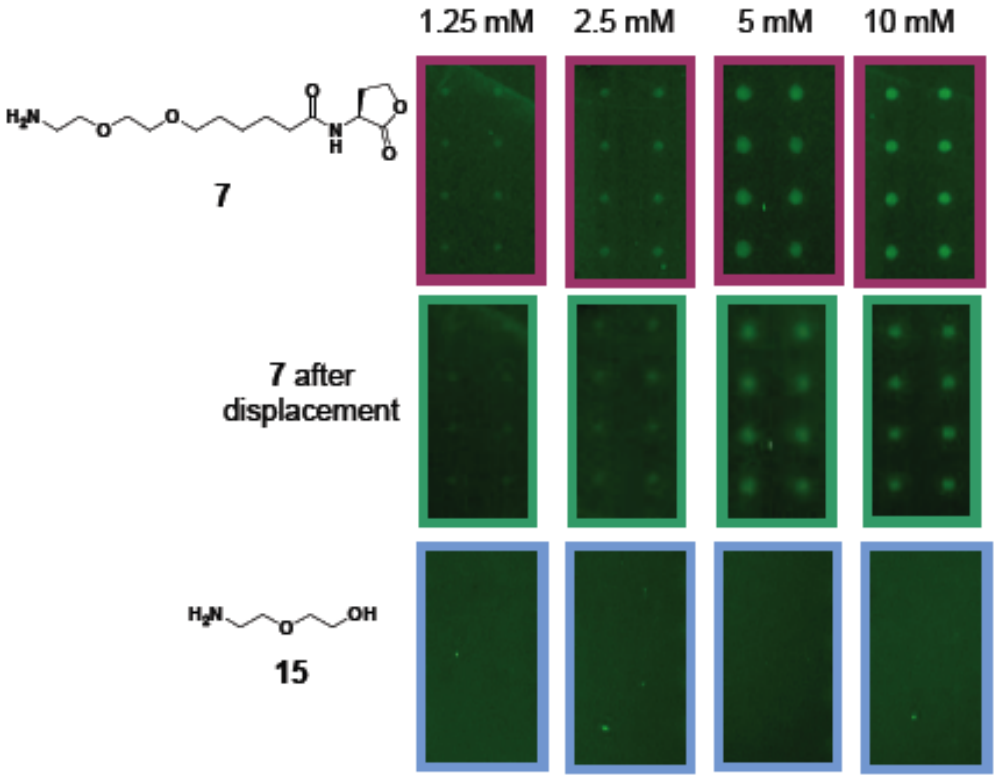

Figure 3 Cy3-CarR-**7** small-molecule microarray screen grabs. **7** and the amino-ethoxy-ethanol **15** were printed at 10, 5, 2.5 and 1.25 mM (8 duplicate spots per concentration) onto a 3D hydrogel slide as outlined in the experimental section of the research paper. Following incubation with Cy3-CarR, the slide was scanned (at 50% PMT) to give the indicated slide images shown at each concentration. The slide was then treated with a solution containing the quorum sensing ligands HHL and OHHL (both at 5 mM) in order to perform a displacement assay to remove the protein from the slide. The slide was finally washed and rescanned (at 50% PMT) to give the Cy3 images for **7** after the displacement.

B2 - Library screening scans

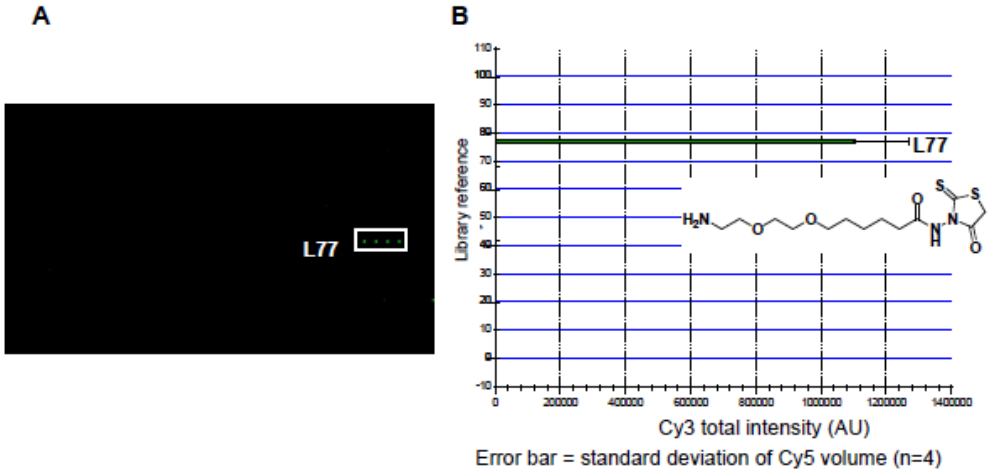

Figure 4 A) Cy3 prescan of a slide printed with the library prior to protein incubation, showing that ligand **L77** generates autouorescence in the Cy3 region. B) Plot of the library reference number versus the pre-scan background corrected Cy3 uorescent intensity. Error bars correspond to standard deviation over 4 replicate spots. AU = arbitrary units

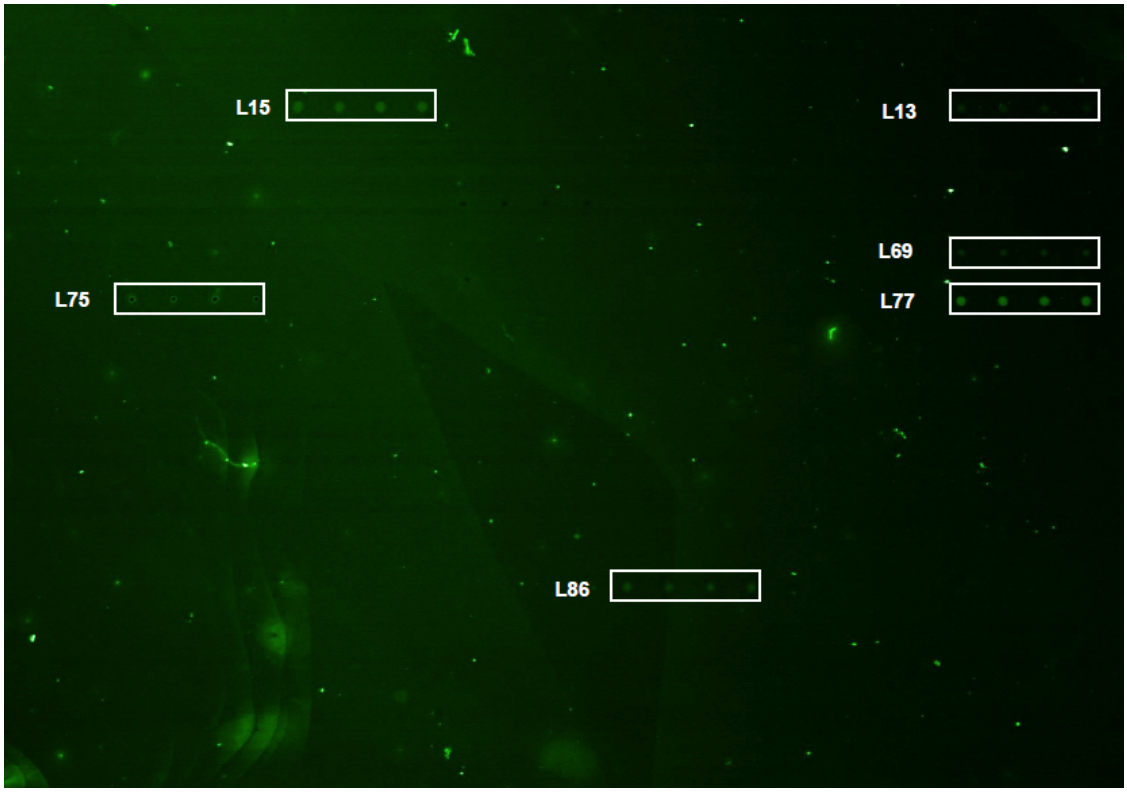

Figure 5 Cy3-CarR/library small-molecule microarray screen. Cy3 scan of the CarR/library microarray. The library was printed (4 duplicate spots per compound) at 10 mM onto a 3D hydrogel slide, then incubated with Cy3-CarR (plus Cy5-avidin) and finally scanned to give the Cy3 image shown. The background corrected Cy3 mean intensities were plotted in Figure 3 of the main paper. Highlighted compounds were visible by qualitative evaluation. **L15** & **L86** were selected as potential hits as they produced the highest fluorescence and had a SNR higher than 3, which is the lower level of accurate detection.

B3 - Concentration Microarray

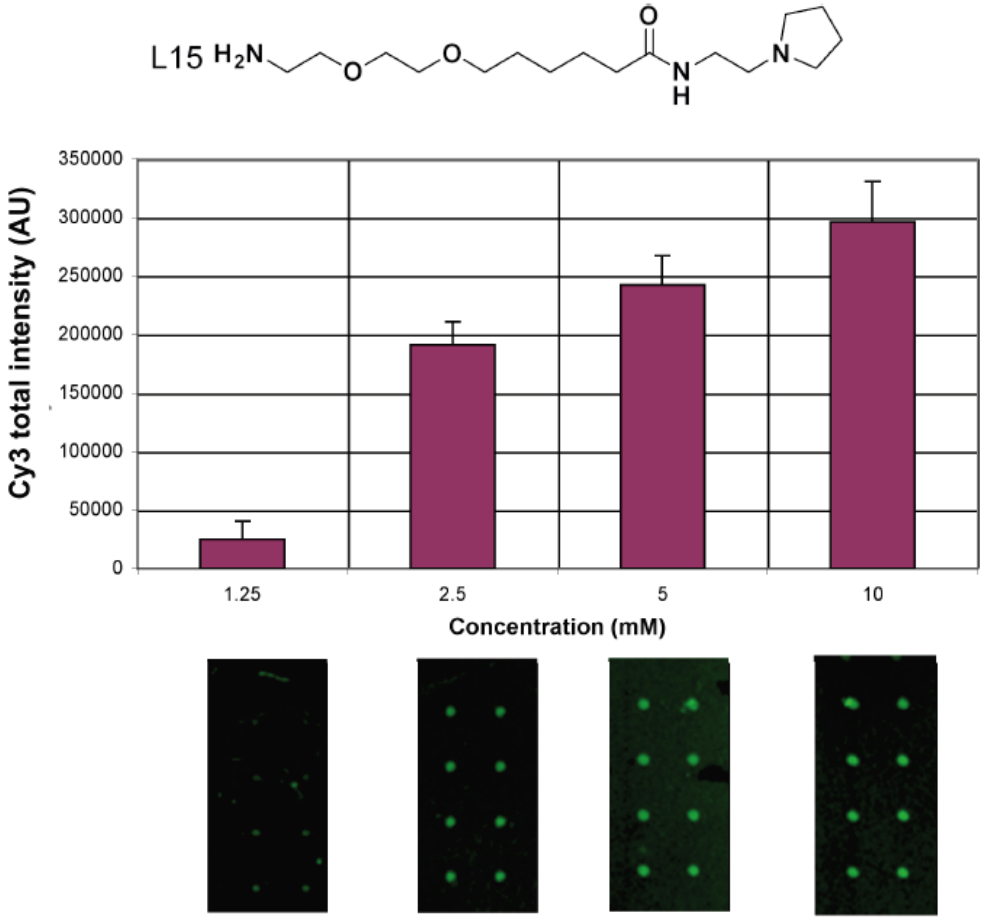

Figure 6 CarR-**L15** background corrected Cy3 total intensity over concentration of printed ligand **L15** and corresponding Cy3 scanned sections. Cy3 intensities based on average across 8 replicate spots and error bars based on standard deviation. AU = arbitrary units.

C – Fluorometric ligand binding assays

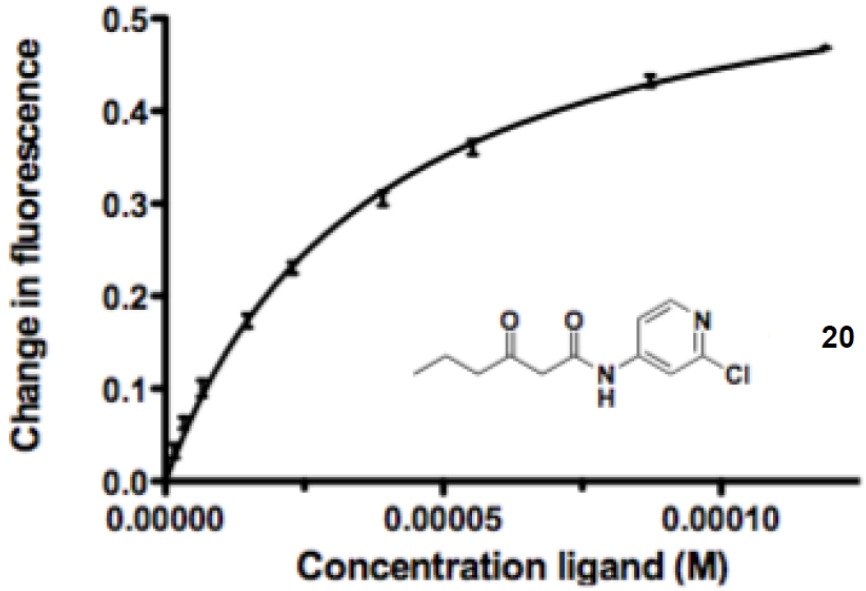

Figure 7 CarR-**20** Fluorometric ligand binding curve (K_d = 37 ± 2.5 μM). Relative change in fluorescence plotted against concentration in Graphpad Prism software using a single binding site model. Error bars correspond to standard deviation across three replicate experiments.

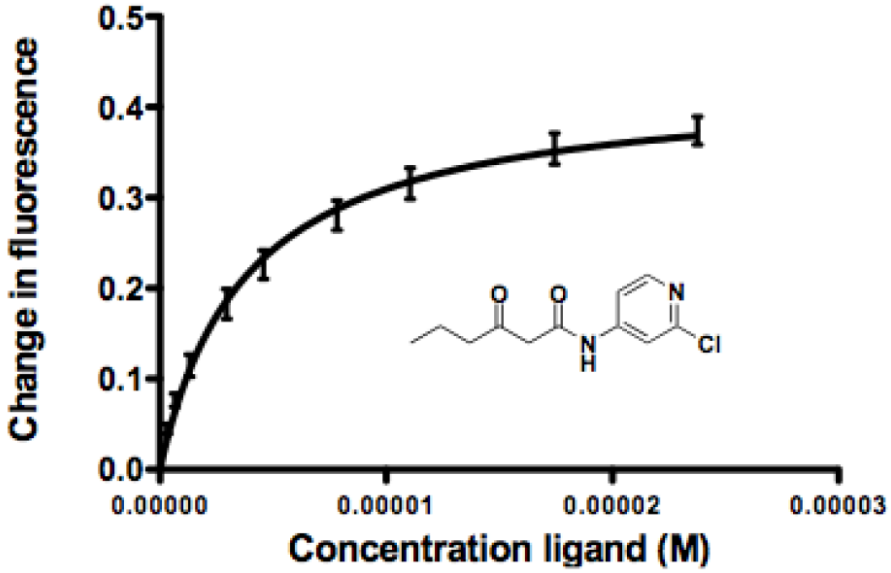

Figure 8 EccR-**20** Fluorometric ligand binding curve (K_d = 3.6 ± 0.2 μM). Relative change in fluorescence plotted against concentration in Graphpad Prism software using a single binding site model. Error bars correspond to standard deviation across three replicate experiments**.**

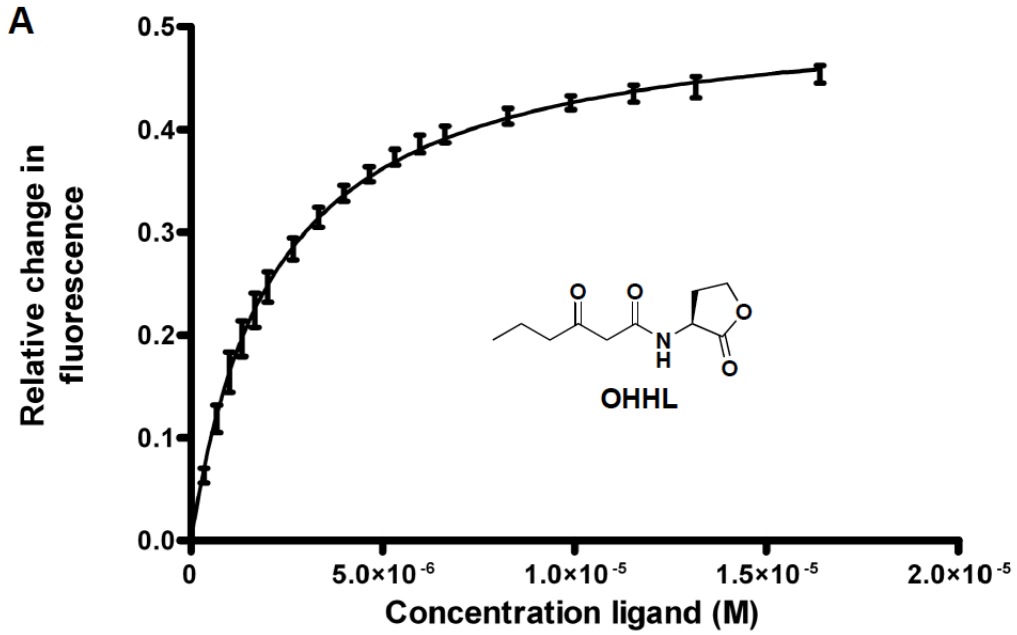

Figure 9 CarR-OHHL Fluorometric ligand binding curve (K_d = 2.0 ± 0.04 μM). Relative change in fluorescence plotted against concentration in Graphpad Prism software using a single binding site model. Error bars correspond to standard deviation across three replicate experiments.

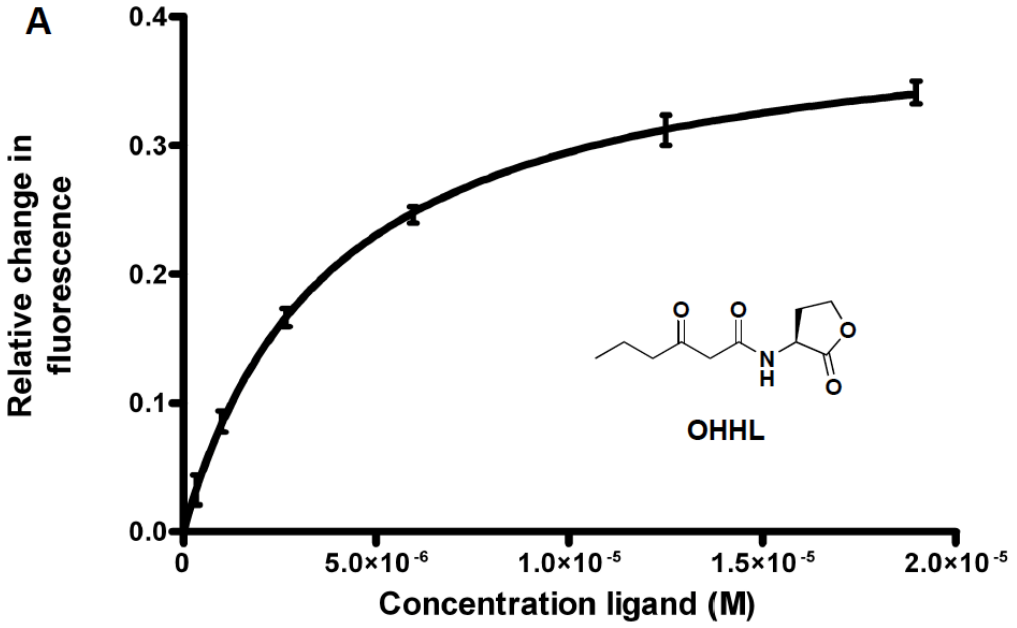

Figure 10 EccR-OHHL Fluorometric ligand binding curve (K_d = 3.9 ± 0.06 μM). Relative change in fluorescence plotted against concentration in Graphpad Prism software using a single binding site model. Error bars correspond to standard deviation across three replicate experiments.

D – ^{1}H-NMR and ^{13}C-NMR spectrum

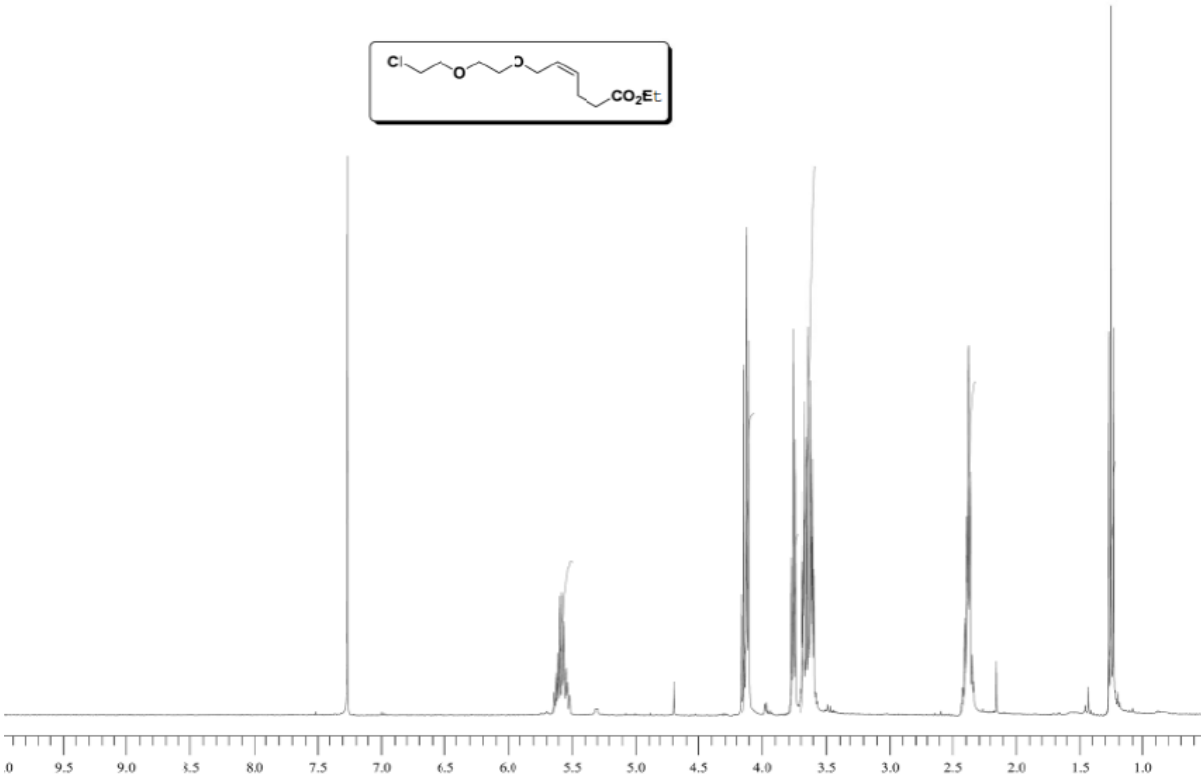

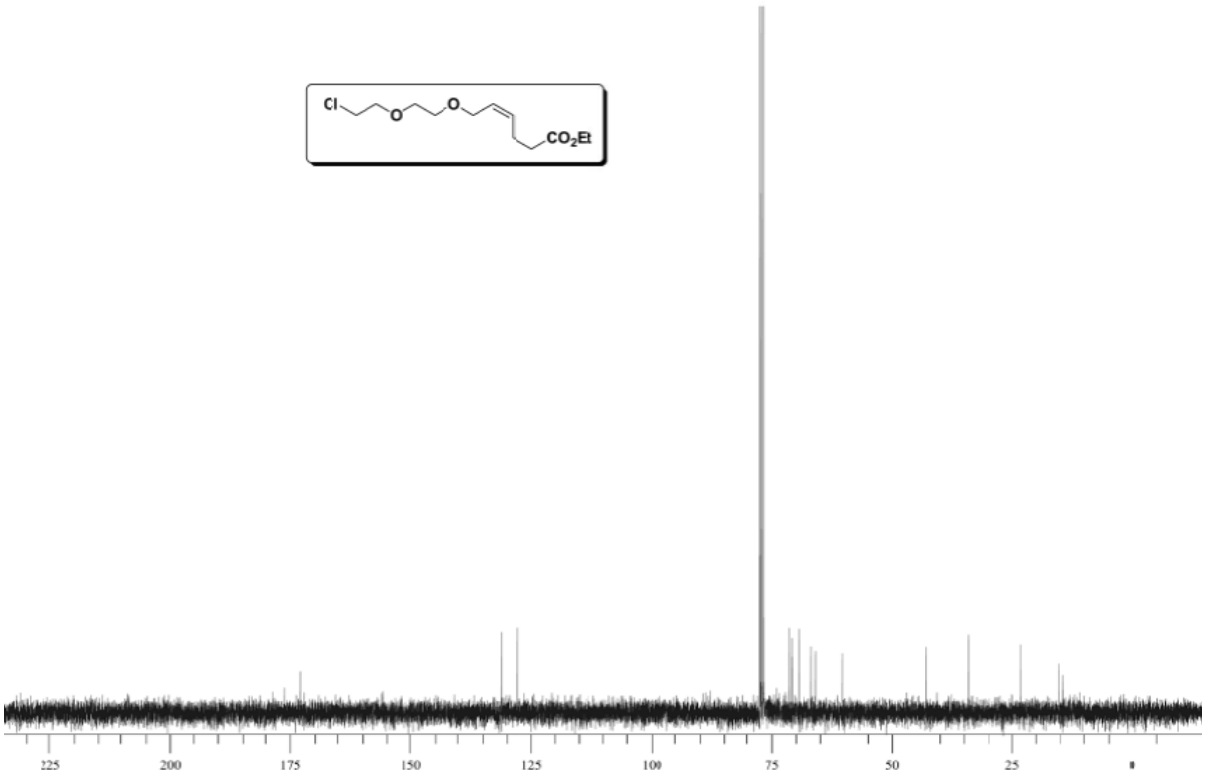

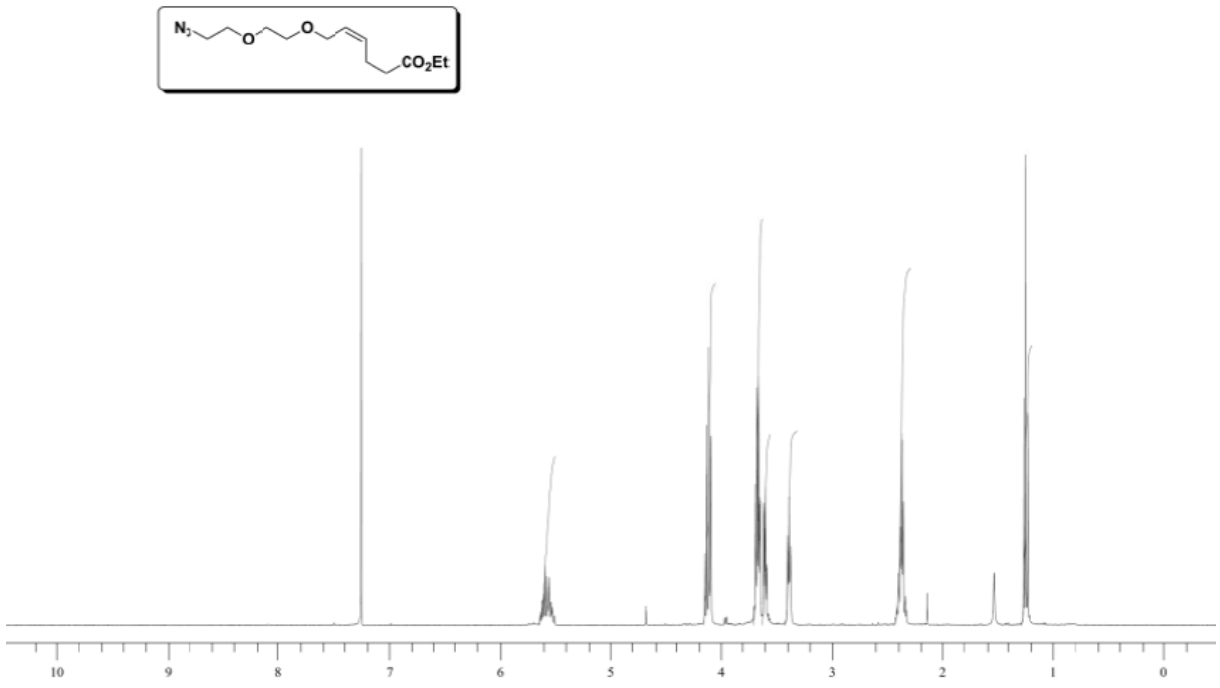
N3
O
O
CO2Et
10
9
8
7
6
5
4
3
2
1
0

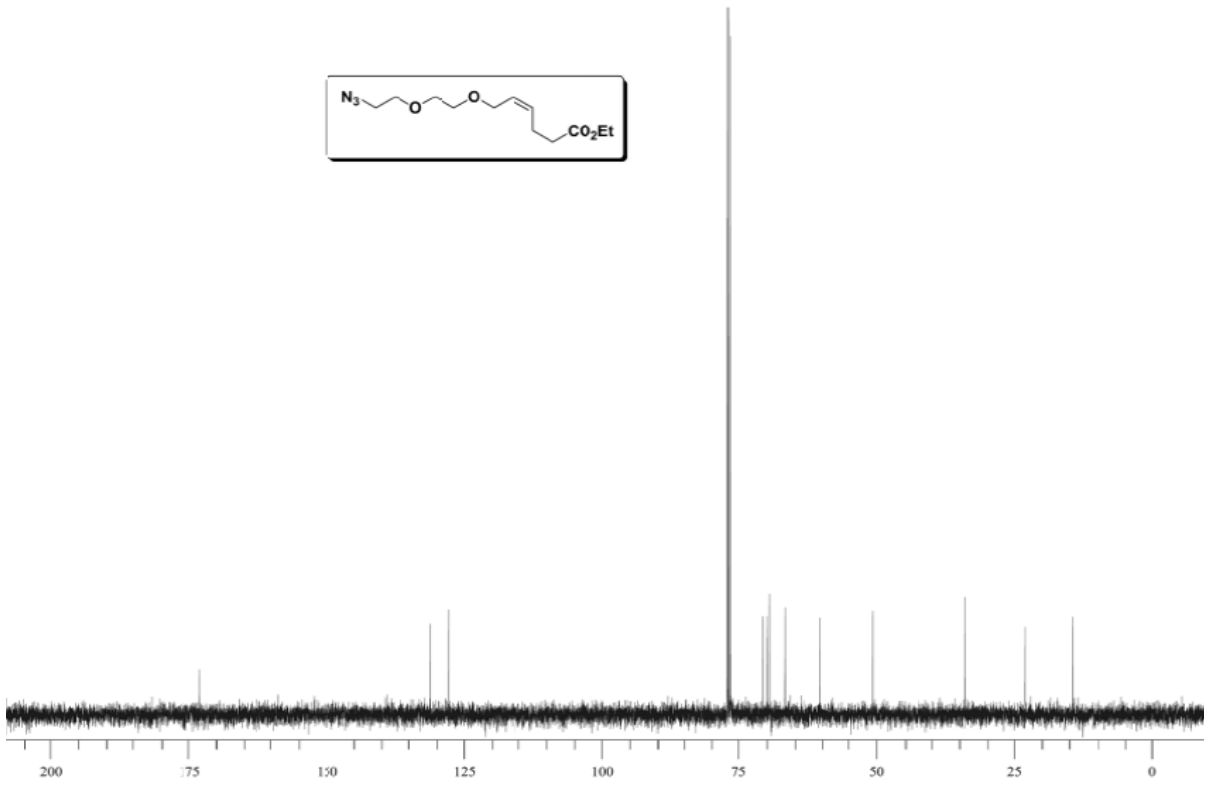
N3
O
O
CO2Et
200
175
150
125
100
75
50
25
0

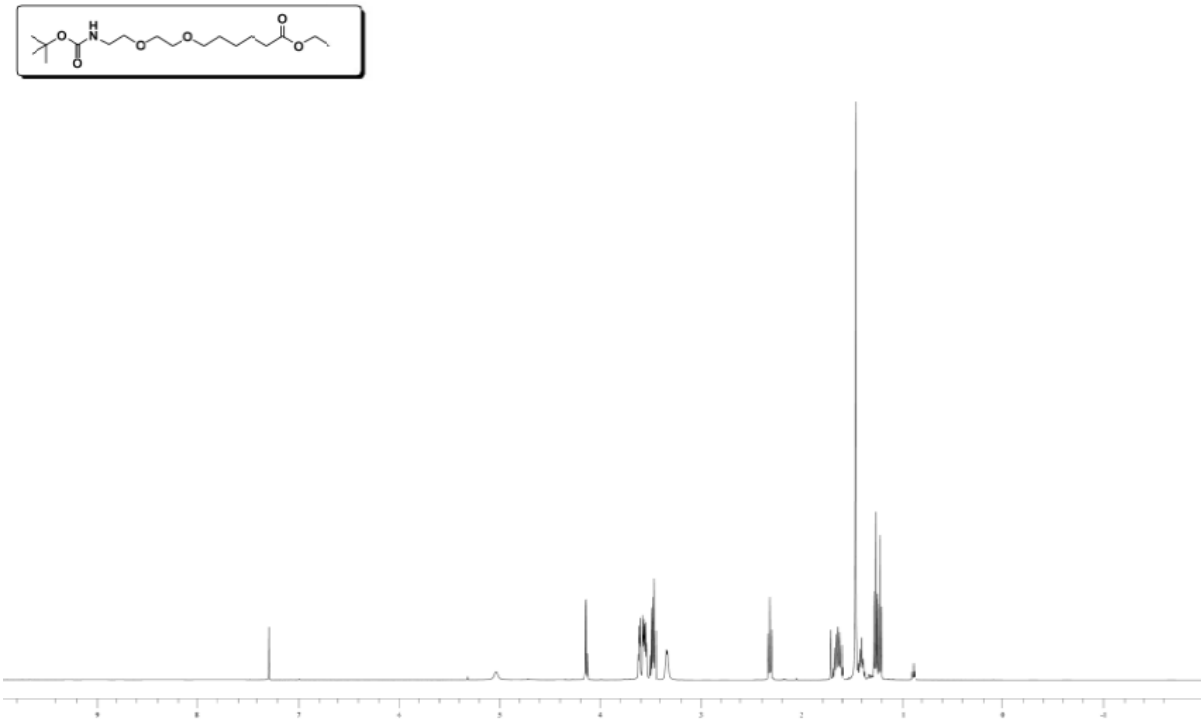

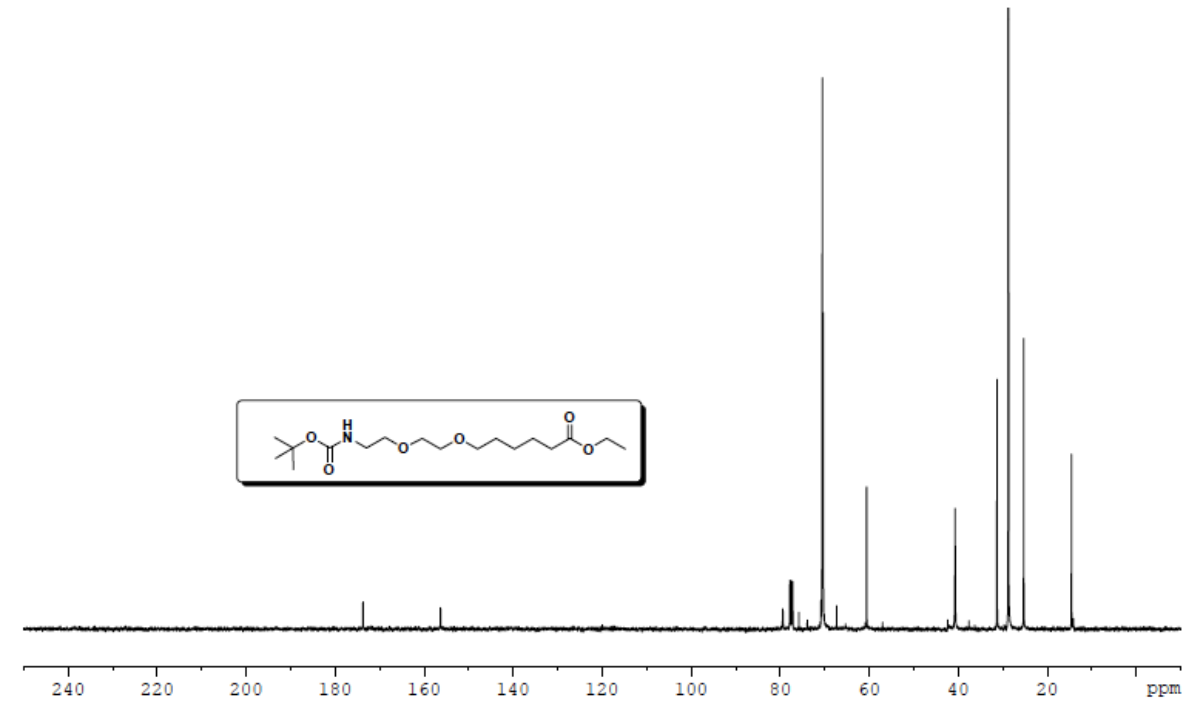
240
220
200
180
160
140
120
100
80
60
40
20
ppm

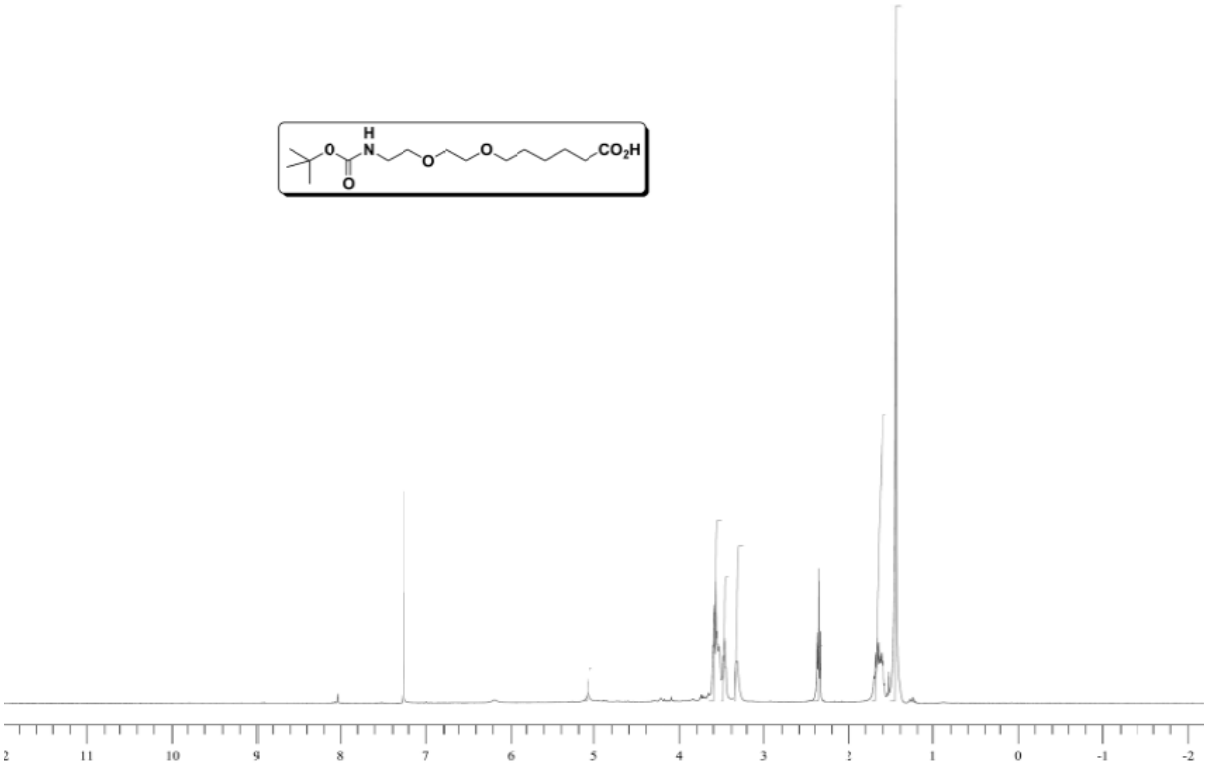
H
N
O
O
O
O
O
O
CO2H
2
11
10
9
8
7
6
5
4
3
2
1
0
-1
-2

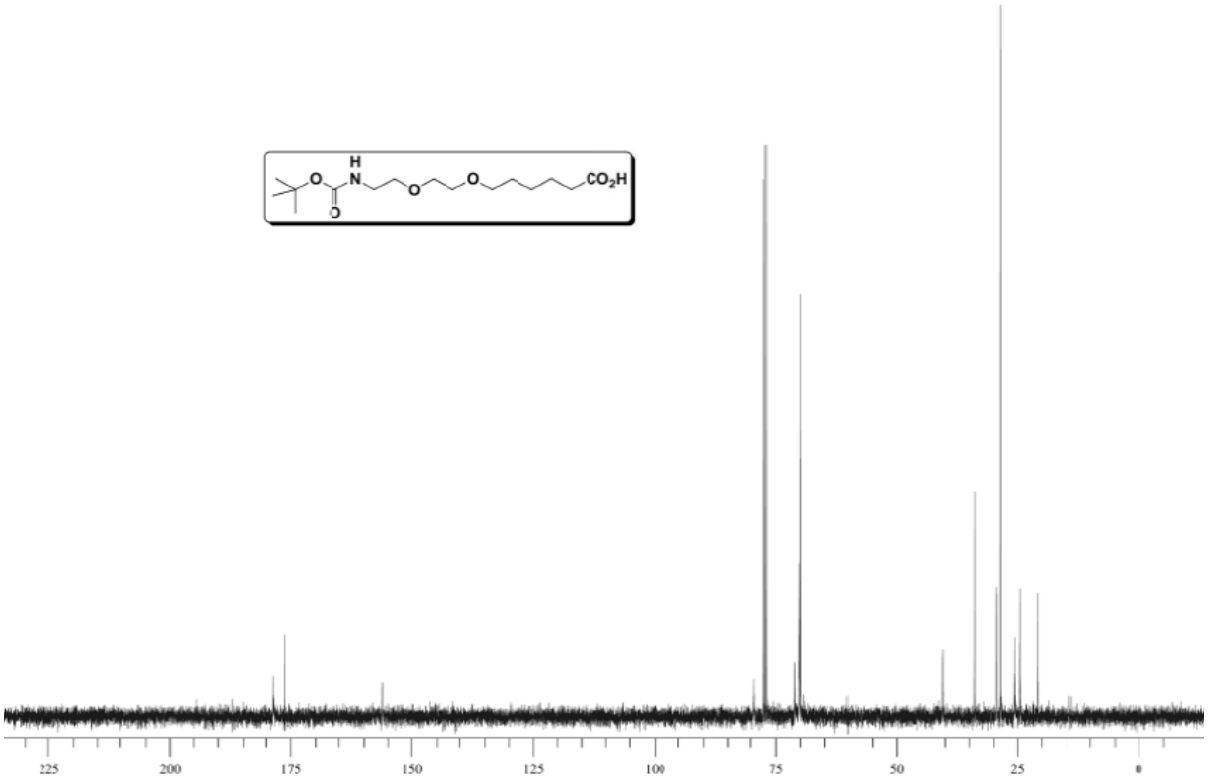
H
N
O
O
O
O
O
O
CO2H
225
200
175
150
125
100
75
50
25
0

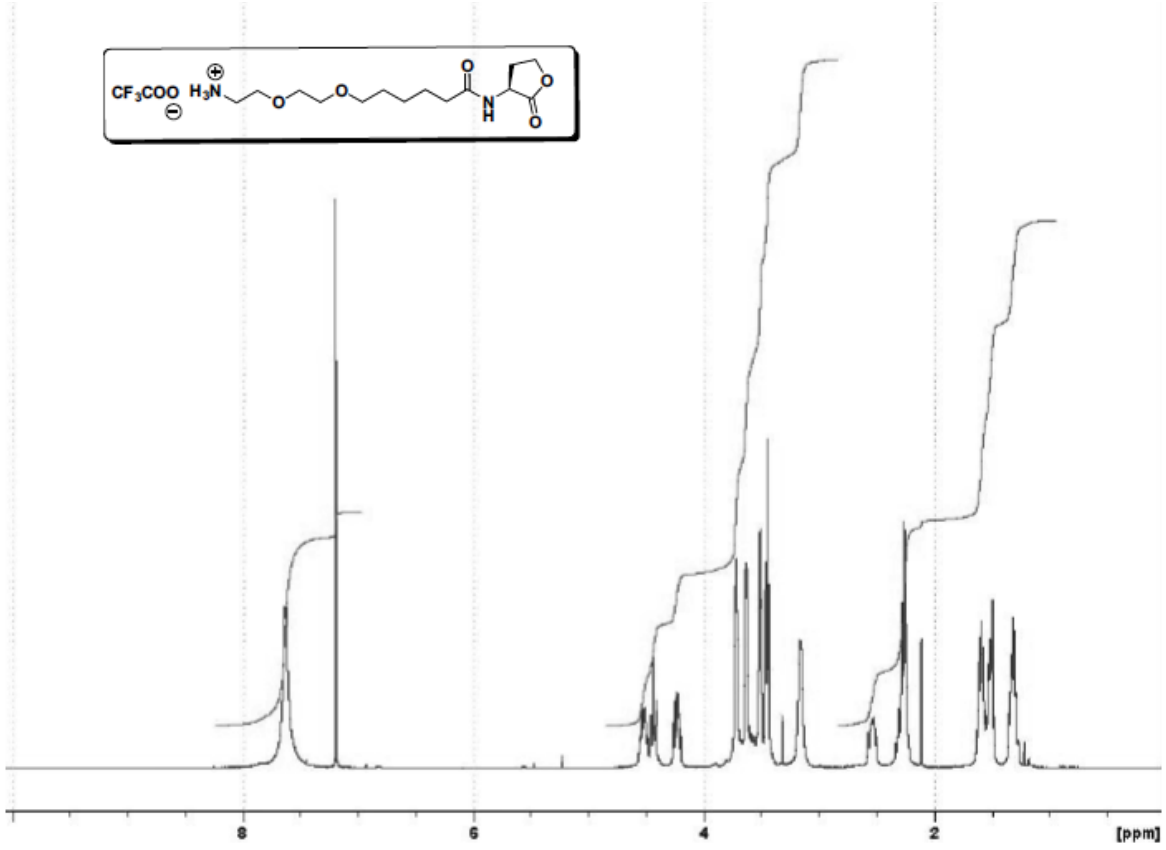
CF3COO
H3N
O
O
O
O
N
H
O
8
6
4
2
[ppm]

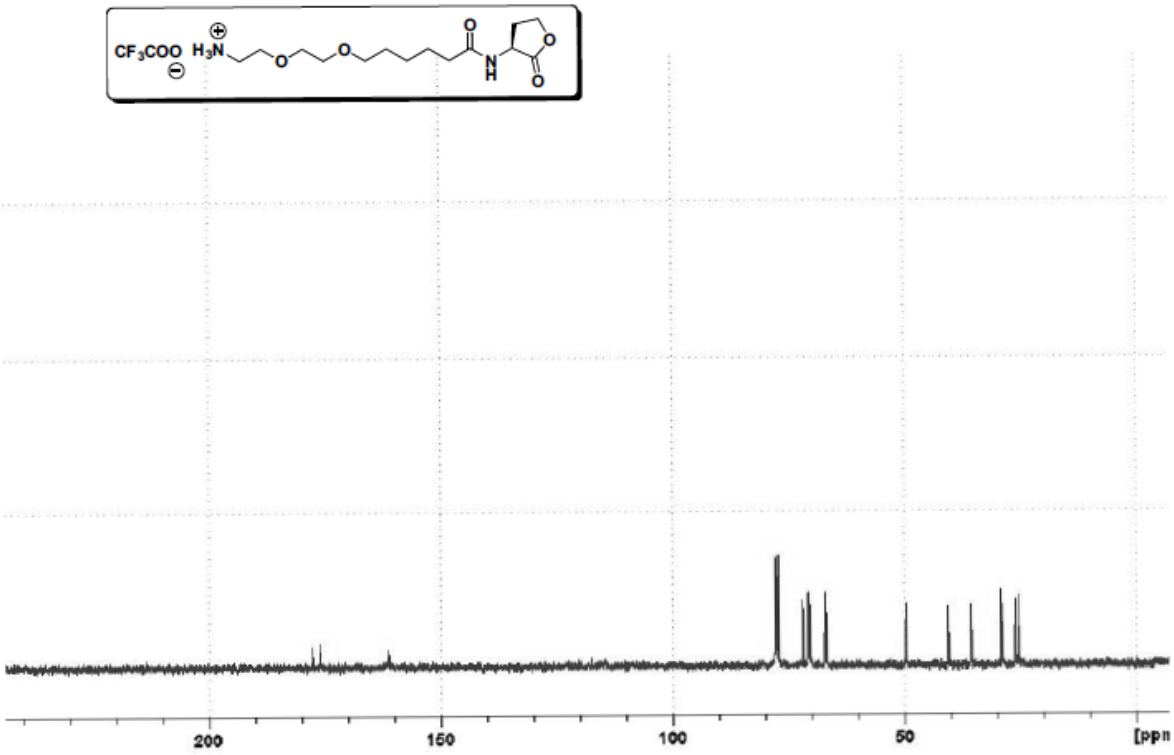
CF3COO
H3N
O
O
O
O
N
H
O
200
150
100
50
[ppm]

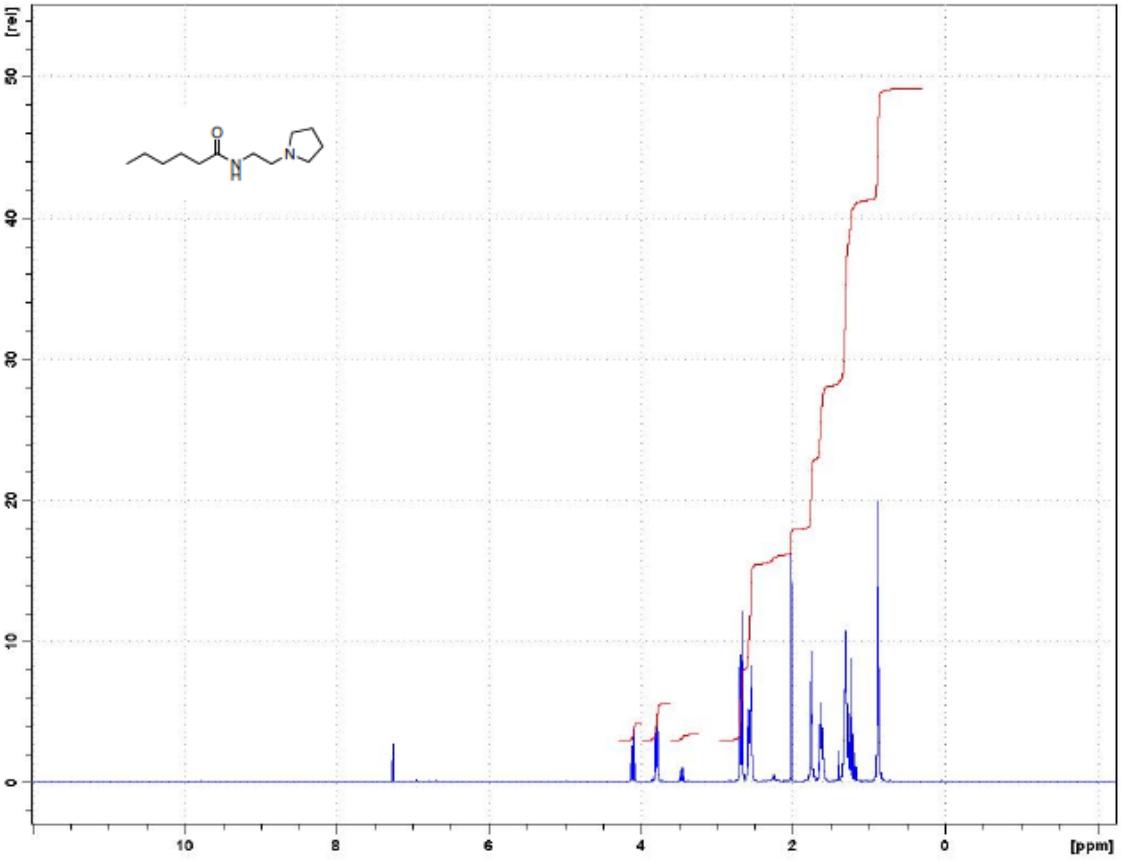
[rel]
50
40
30
20
10
0
10
8
6
4
2
0
[ppm]
O
N
H
N

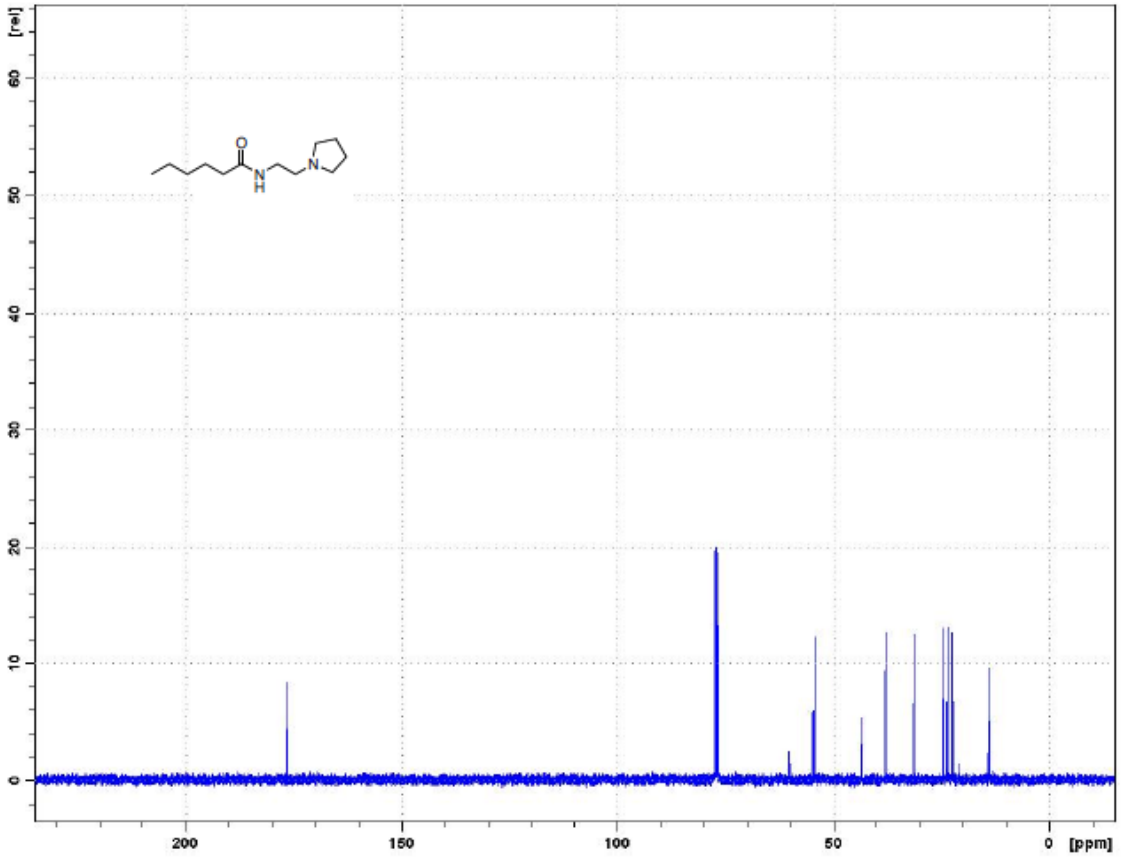
[rel]
60
50
40
30
20
10
0
200
150
100
50
0
[ppm]
O
N
H
N

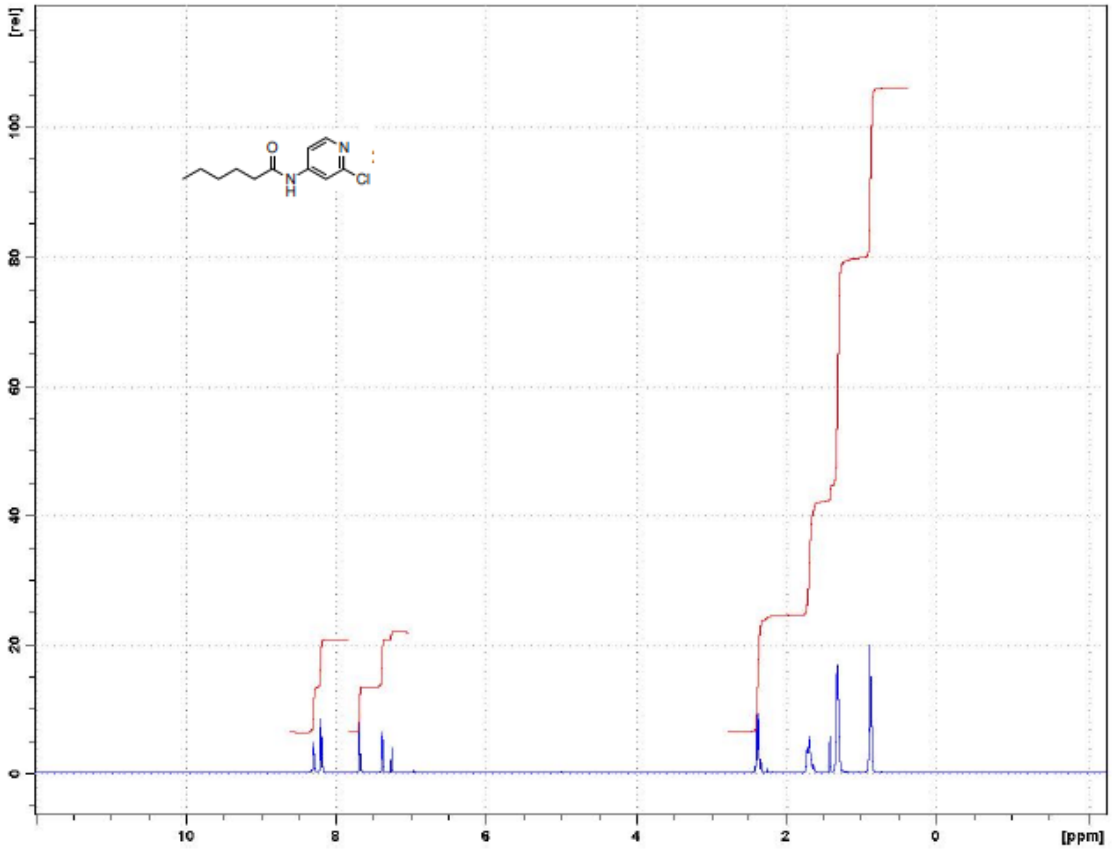
[rel]
100
80
60
40
20
0
10
8
6
4
2
0
[ppm]
O
N
H
Cl

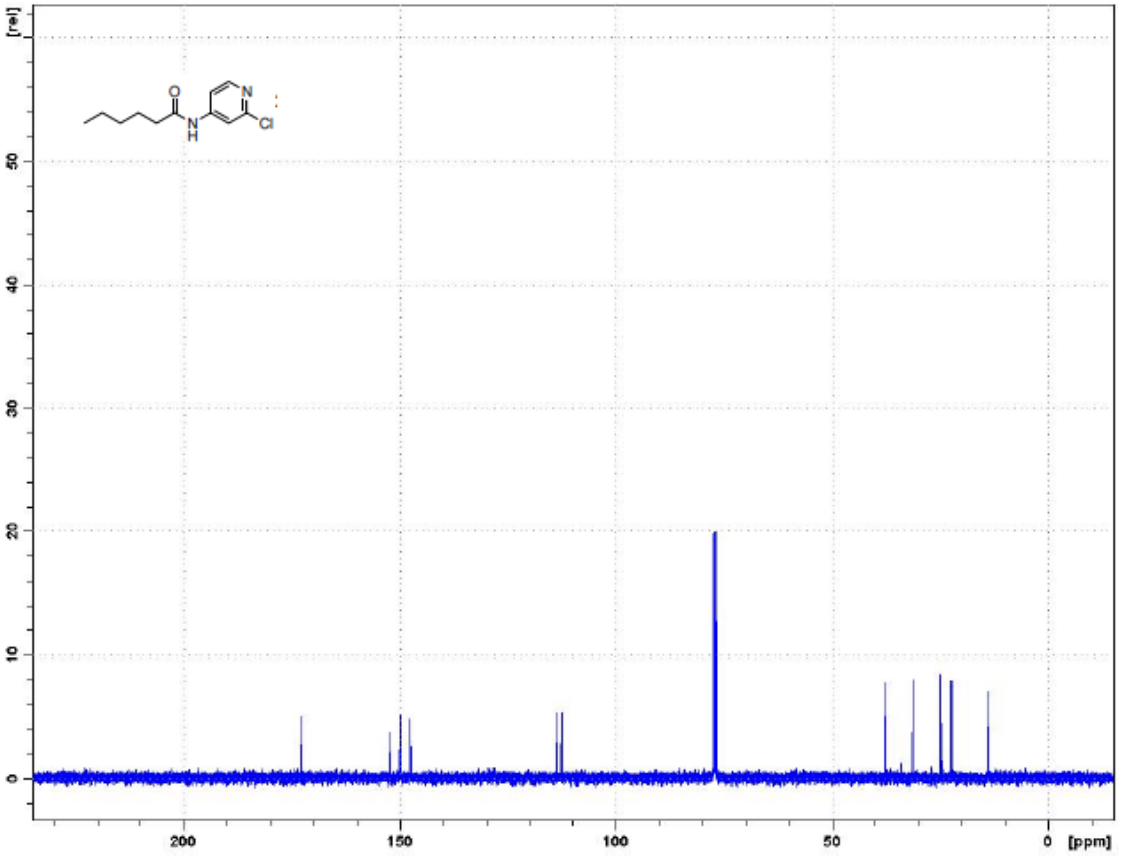
[rel]
50
40
30
20
10
0
200
150
100
50
0
[ppm]
O
N
H
Cl

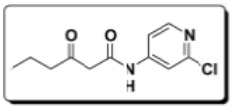
O
O
N
H
Cl

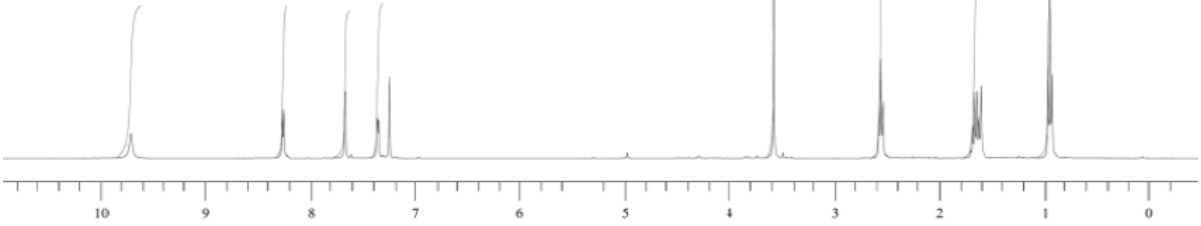
10
9
8
7
6
5
4
3
2
1
0

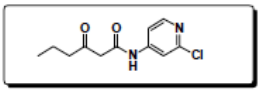
O
O
N
H
Cl

225
200
175
150
125
100
75
50
25
0

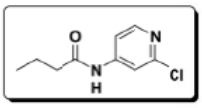
O
N
N
H
Cl

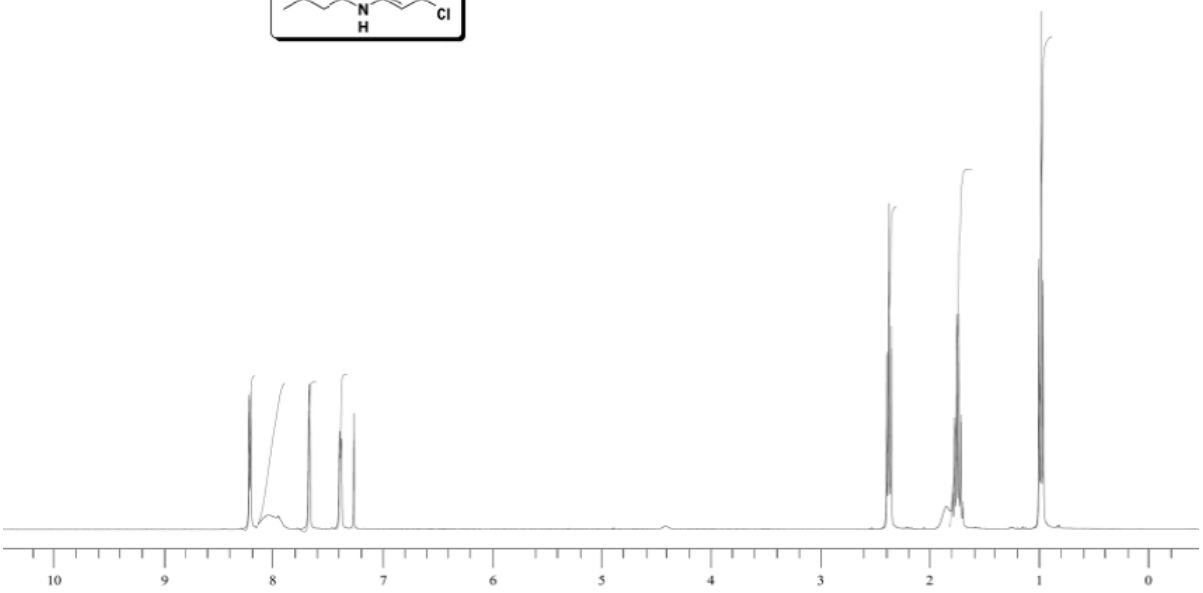
10
9
8
7
6
5
4
3
2
1
0

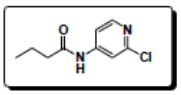
O
N
N
H
Cl

225
200
175
150
125
100
75
50
25
0

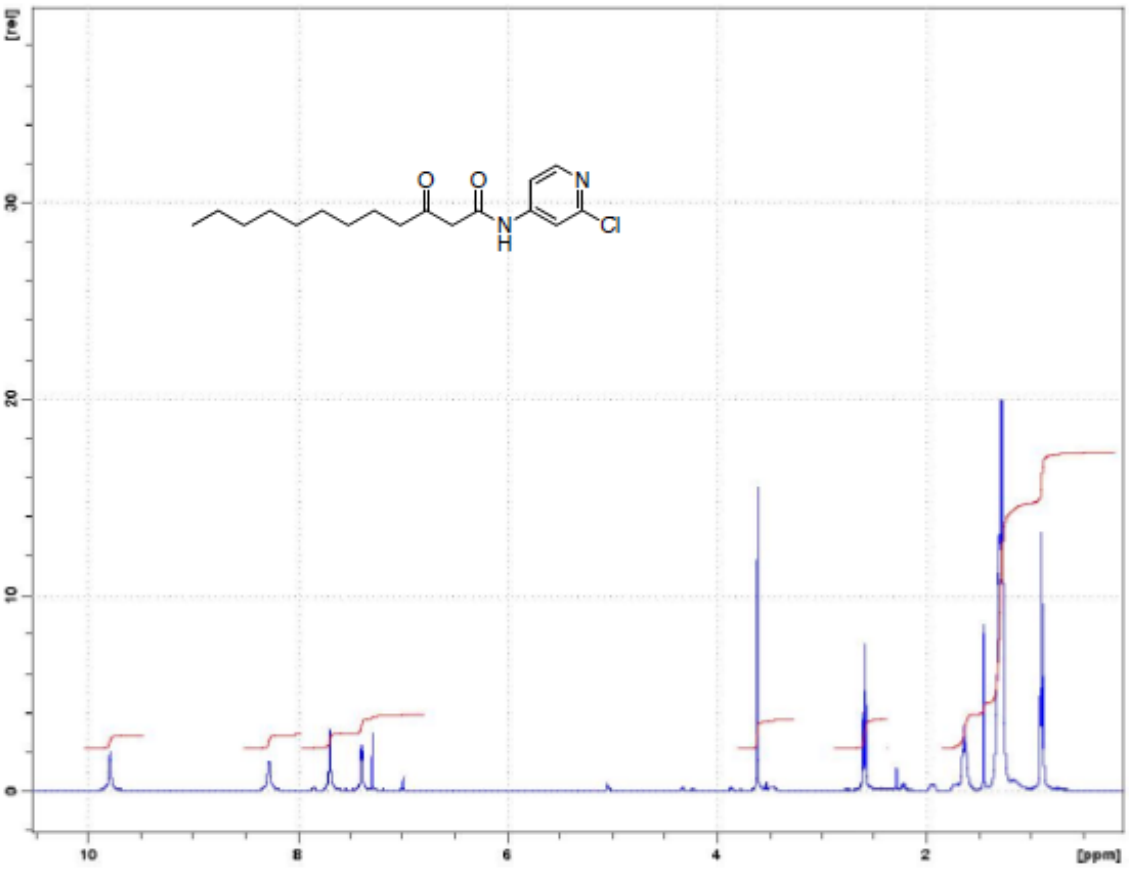
[rel]
30
20
10
0
O
O
N
H
N
Cl
10
8
6
4
2
[ppm]

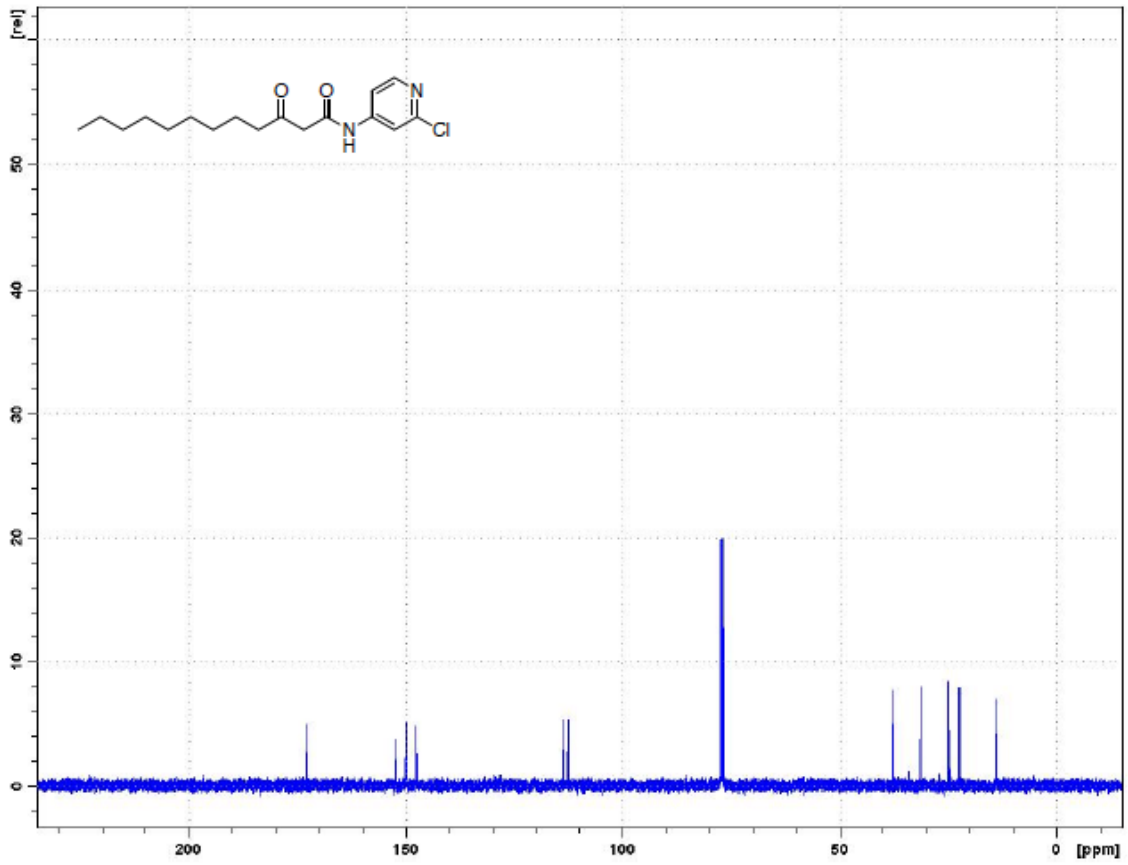
[rel]
50
40
30
20
10
0
O
O
N
H
N
Cl
200
150
100
50
0
[ppm]

E – Growth curves with LIS

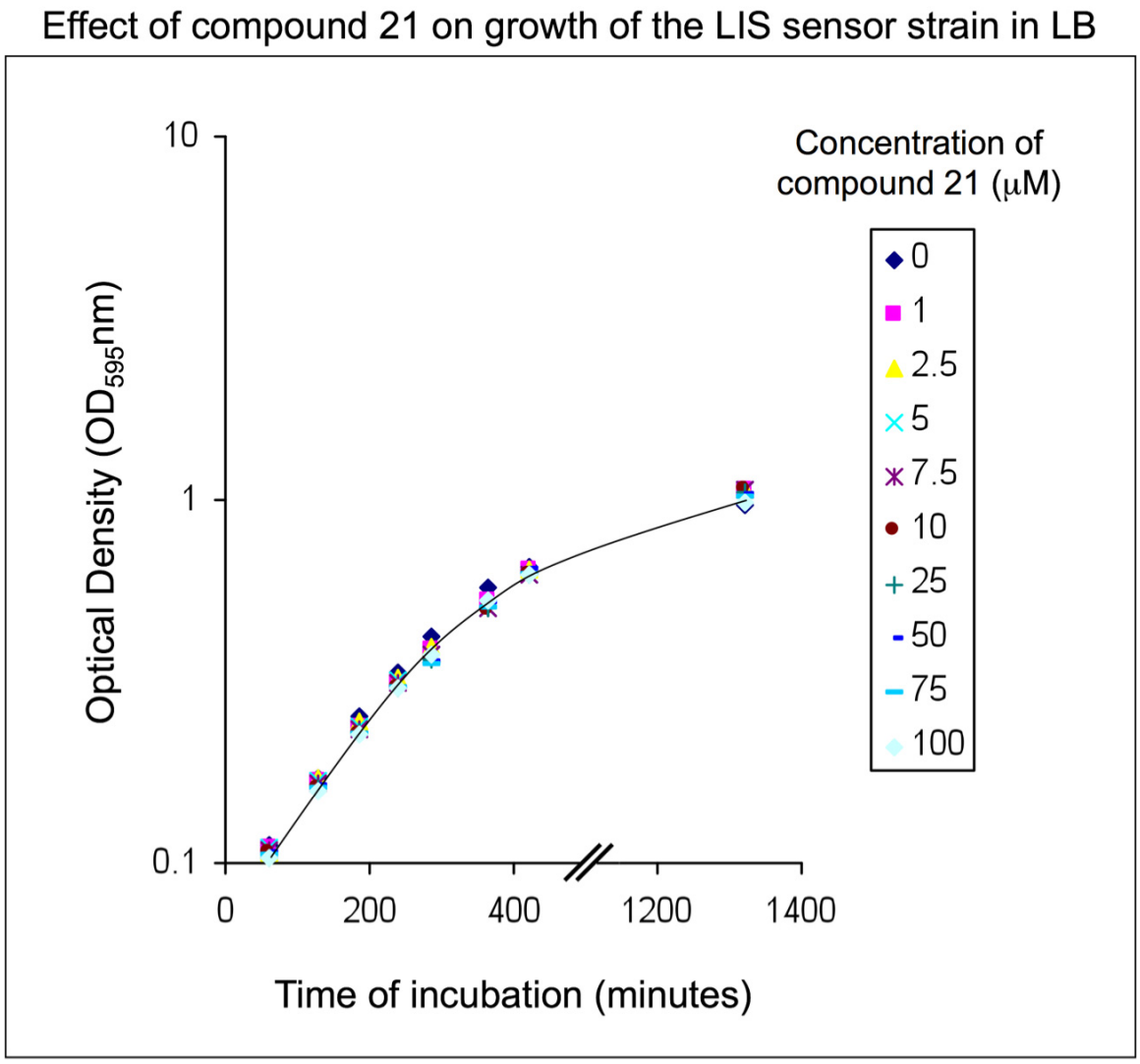

F – Action of compound 21 with wild type Serratia

Effect of compound 21 on pigment production by wild-type ATCC39006